Stable Radio Frequency Dissemination With Phase Conjugation

Blanca Mir and Víctor Pina
Bachelor's degree in Engineering Physics
Universitat Politècnica de Catalunya (UPC)
(Dated: June 4, 2021)

Fiber-optic frequency transfer is a promising option for stable and long-distance radio frequency (RF) transmission. This paper consists on a proposed operation principle and simulation of a stable frequency dissemination scheme using photonic microwave phase conjugation.

I. INTRODUCTION

Social and scientific applications require ultra-stable frequency dissemination. Fiber-optic frequency transfer is a promising way for stable and long-distance radio frequency (RF) transmission, compared to satellite links, because of lower attenuation, larger bandwidth, higher stability and immunity to electromagnetic interference.

Ultrastable RF long-distance dissemination has important applications such as particle accelerators, synchronisation and comparison of remote clocks, radio astronomy, navigation, gravitational-waves detection and very long baseline interferometry (VLBI) .

The phase of the optical transmitted signal is subject to random changes in temperature and mechanical vibration that modify the propagation delay of the fiber-optic links and, hence, add extra phase noises. In order to cancel the phase drift, principles of round-trip phase compensation have been proposed. Compensation techniques are often based on returning a light signal along the optical path and correcting the phase shift.

RF transfer schemes include two different types of compensation methods [1]. Active compensation scheme typically uses the phase error from a round-trip probe signal. It allows to achieve very high phase stability, however, the response velocity and phase recovery time are limited. Passive compensation scheme is based on frequency mixing. It allows to perform a rapid and endless phase fluctuation compensation, and get rid of phase error detection and feedback circuits. Mixers generate some local oscillator leakage and harmonics interference that might reduce the phase stability.

In this work, we have considered the RF transfer principle suggested in [1] and we have simulated it.

II. THEORETICAL OVERVIEW

A. Mach-Zehnder Interferometer

RF transfer active compensation schemes make use of Mach-Zehnder modulators (MZM). Firstly, the optical input is divided into two arms. Electric signals are applied so as to change its path length, resulting in a phase modulation. After that, the signal is once again recombined into a modulated optical output.

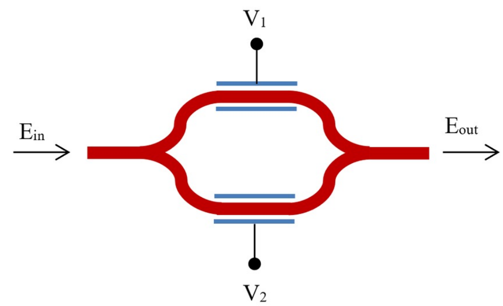

FIG. 1. Mach-Zehnder modulator structure. [9]

If we assume that the optical field inserted into the device is equally divided between the upper and lower arms (*push-pull*), we obtain the following equation

$$E_{out} = E_{in} \cos(\frac{\pi}{2}\frac{V}{V_\pi}) \tag{1}$$

where V_π is the halfway voltage and V the applied voltage.

We can define two angular parameters, which will allow us to determine the working point in the device's transfer function with more ease. By making use of them and assuming a sinusoidal voltage wave with both DC and AC components (even though the former will commonly be eliminated by using a bias tee, which separates them by using an inductor and a capacitor), we have the following

$$V(t) = V_B + V_{RF}\cos(\omega_{RF} t) \tag{2}$$

$$\theta_B = \frac{\pi V_B}{V_\pi} \qquad m = \frac{\pi V_{RF}}{V_\pi} \tag{3}$$

where θ_B is known as the angle bias and m is the modulation parameter.

Furthermore, in order to use the MZM for different purposes, it is important to define our θ_B so as to choose the device's transfer working point. Primarily, there are two relevant choices: the quadrature point, which corresponds to $\theta_B = \frac{\pi}{2}$ and null point, for an $\theta_B = \frac{\pi}{4}$.

If we assume that the loss for each arm is not equal, a new parameter should be considered, the extinction ratio (ER). Therefore, the field relation can be expressed as

$$E_{out} = \frac{1}{2}\left[\exp\left(j\frac{\theta_B + m\cos(\omega_{RF}t)}{2}\right) + \gamma\exp\left(-j\frac{\theta_B + m\cos(\omega_{RF}t)}{2}\right)\right] \quad (4)$$

where γ is a parameter ranging from 0 to 1 related to ϵ as

$$\gamma = \frac{\sqrt{ER} - 1}{\sqrt{ER} + 1} \quad (5)$$

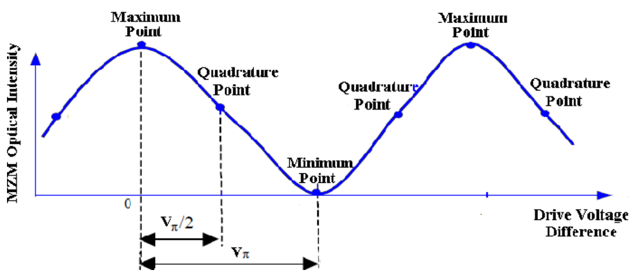

FIG. 2. Mach-Zehnder's transfer function. [10]

B. Characterization of Frequency Stability

Allan variance [2] was developed to quantify the frequency stability in time domain and is expressed as $\sigma_y^2(\tau)$. Allan deviation is the square root of the Allan variance, $\sigma_y(\tau)$. A low Allan variance means a good stability over the measured period.

The Allan deviation is computed from a series of consecutive frequency measurements obtained by averaging over a period of time τ. Typically, the signal from a frequency source is expressed as

$$V(t) = V_0 \cos[2\pi\nu_0 t + \varphi(t)] \quad (6)$$

where V_0 is the amplitude of the signal, ν_0 is the nominal center frequency of the signal and $\varphi(t)$ is considered as the time-varying deviations from the nominal phase $2\pi\nu_0 t$. The instantaneous fractional frequency deviation from the nominal center frequency is given by

$$y(t) = \frac{1}{2\pi\nu_0}\frac{d}{dt}\varphi(t) \quad (7)$$

The Allan variance for an averaging time τ is defined as

$$\sigma_y^2(\tau) = \left\langle \frac{1}{2}[\bar{y}(t+\tau) - \bar{y}(t)]^2 \right\rangle \quad (8)$$

where $\bar{y}(t)$ is the time average of $y(t)$ over the period τ. $\sigma_y(t)$ can be estimated from a finite set of N consecutive average values of the center frequency ν_i.

$$\sigma_y(\tau) \approx \left[\frac{1}{2(N-1)\nu_0^2}\sum_{i=1}^{N-1}(\bar{\nu}_i - \bar{\nu}_{i+1})^2\right]^{1/2} \quad (9)$$

III. OPERATION PRINCIPLE

The schematic diagram of the proposed remote RF phase stabilization with passive compensation involving phase conjugation is illustrated in Fig.3.

Mathematically, the RF signal generated by a microwave source (MS) can be expressed as

$$V_1 = \cos(\omega_0 t + \varphi_0) \quad (10)$$

where ω_0 and φ_0 stand for the angular frequency and initial phase, respectively. V_1 modulates an optical carrier obtained from a laser diode (LD) at the Mach-Zehnder modulator (MZM1) biased at the null point. Through an optical filter (TOF1), the two first-order optical sidebands (OSBs) are selected out, and they can be expressed as

$$E_1 \propto e^{i\omega_c t} \cdot \left[e^{-i(\omega_0 t + \varphi_0)} + e^{i(\omega_0 t + \varphi_0)}\right] \quad (11)$$

where ω_c is the angular frequency of the optical carrier and the initial phase is assumed to be zero. The two first-order optical sidebands form the desired two-tone optical carrier.

Afterwards, E_1 is divided into two branches through an optical coupler (OC1). One branch is detected by a photodetector (PD1) and a frequency-doubled RF signal is obtained, which is written as

$$V_2 \propto \cos[2(\omega_0 t + \varphi_0)] \quad (12)$$

Taking into consideration the other branch, the two-tone optical carrier is transmitted along the single-mode fiber (SMF1) to the first remote site where the 2 x 2 0C2 couples out a forward transferred optical signal which is written as

$$E_2 \propto e^{i\omega_c(t-\tau_1)} \cdot \left[e^{-i(\omega_0 t + \varphi_0 - \varphi_1)} + e^{i(\omega_0 t + \varphi_0 - \varphi_1)}\right] \quad (13)$$

where $\varphi_1 = \omega_0\tau_1$ is the accumulation phase fluctuation that corresponds to the propagation delay, τ_1, of SMF1.

The other optical signal that has been coupled out is injected into SMF2 and returns to the local site as a round-trip probe signal (E_3) that can be expressed as

$$E_3 \propto e^{i\omega_c(t-\tau_s)} \cdot \left[e^{-i(\omega_0 t + \varphi_0 - \varphi_s)} + e^{i(\omega_0 t + \varphi_0 - \varphi_s)}\right] \quad (14)$$

where $\tau_s = \tau_1 + \tau_2$ is the propagation delay corresponding to the entire fiber link and $\varphi_s = \omega_0\tau_s = \varphi_1 + \varphi_2$ is the phase change. The phase fluctuation of SMF2 with propagation delay τ_2 is expressed as $\varphi_2 = \omega_0\tau_2$.

E_3 is modulated by the signal V_2 at the Mach-Zehnder modulator biased at the null point (MZM2) where the two optical carriers are removed. Fig.4 shows the spectrum evolution of the modulation procedure described.

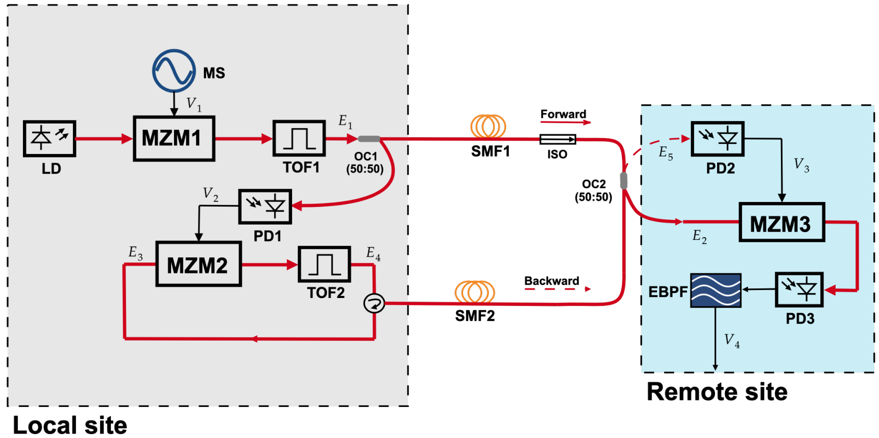

FIG. 3. The schematic diagram of the proposed dissemination of stabilized frequency-quadruple RF signal over a fiber loop link with passive compensation. MS: microwave source, LD: laser diode, MZM: Mach-Zehnder modulator, TOF: tunable optical fiber, PD: photodetector, OC: optical coupler, ISO: isolator, EBPF: electrical bandpass filter, SMF: single-mode fiber. (Image reproduced from [1])

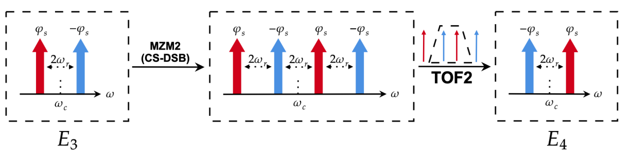

FIG. 4. Spectrum evolution of phase conjugation from the implementation of the second MZM (MZM2). (Image reproduced from [1])

Four first-order optical sidebands are generated after modulation at MZM2, neglecting high-order optical sidebands. Since the frequency spacing of the two optical carriers of E_3 is $2\omega_0$, that is, the frequency of the modulated signal V_2, the two first-order optical sidebands in the middle experiment phase exchange. After that, the two first-order sidebands are filtered out by TOF2. The final optical signal E_4 can be written as

$$E_4 \propto e^{i\omega_c(t-\tau_s)} \cdot \left[e^{-i(\omega_0 t+\varphi_0+\varphi_s)} + e^{i(\omega_0 t+\varphi_0+\varphi_s)}\right] \quad (15)$$

The RF signal carried on E_4 is a conjugate signal relative to that on E_3 in terms of φ_s. Therefore, phase conjugation is achieved, and no electrical mixers or other microwave sources have been used.

The phase-conjugated signal E_4 is transmitted back to the remote site along a single-mode fiber (SMF2). The forward and backward signals propagated along SMF2 would undergo the same propagation delay. Afterwards, the backward signal is coupled out by OC2 and E_5 is extracted. E_5 can be expressed as

$$\begin{aligned} E_5 &\propto e^{i\omega_c(t-\tau_2-\tau_s)} \cdot \left[e^{-i(\omega_0 t-\varphi_2+\varphi_0+\varphi_s)} + e^{i(\omega_0 t-\varphi_2+\varphi_0+\varphi_s)}\right] \\ &= e^{i\omega_c(t-\tau_2-\tau_s)} \cdot \left[e^{-i(\omega_0 t+\varphi_1+\varphi_0)} + e^{i(\omega_0 t+\varphi_1+\varphi_0)}\right] \end{aligned} \quad (16)$$

E_5 is photodetected by PD2, then, the phase-conjugated RF signal is

$$V_3 \propto \cos[2(\omega_0 t + \varphi_0 + \varphi_1)] \quad (17)$$

At the MZM3 biased at a quadrature point, V_3 modulates the forward signal E_2 that carries a RF signal with frequency of $2\omega_0$ and phase change $-2\varphi_1$.

$$\begin{aligned} E_6 \;&\propto e^{i(\omega_0 t-\varphi_1+\varphi_0)} + e^{i(-\omega_0 t+\varphi_1-\varphi_0)} \\ &+e^{i(3\omega_0 t+\varphi_1+3\varphi_0)} + e^{i(-3\omega_0 t-\varphi_1-3\varphi_0)} \end{aligned} \quad (18)$$

The two optical carriers at its input are not suppressed, and even though modulation sidebands of one carrier will fall on the frequency corresponding to the other carrier, under the small-signal approximation we will consider the carriers don't significantly change their value. Additional sidebands at $2\omega_r$ from each carrier will beat with the other carrier generating an electrical frequency at $4\omega_r$.

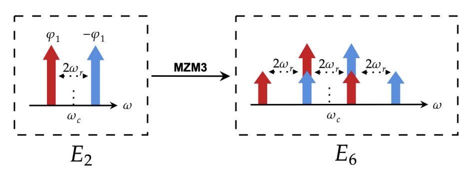

FIG. 5. Spectrum evolution of phase conjugation from the implementation of the MZM at quadrature-point (MZM3). (Image reproduced from [1])

After photomixing at PD3, the phase fluctuation $-2\varphi_1$ of the electrical signal carried by E_2 and $2\varphi_1$ of the RF signal V_3 are compensated.

Hence, the term of sum frequency corresponding to the mixing product is filtered out by an electrical bandpass filter (EBPF) and expressed as

$$V_4 \propto \cos[4(\omega_0 t + \varphi_0)] \quad (19)$$

One can observe that the frequency and phase have been multiplied by 4 with respect to those of the standard

RF signal V_1. Therefore, the stable quadruple frequency dissemination with photonic microwave phase conjugation has been successfully modelled.

IV. SIMULATION AND DISCUSSION

Computer simulation with **MATLAB** is performed to prove the viability of the scheme explained in the previous section. In our simulation system, the frequency of the standard reference signal is set at 1 GHz and the initial phase of the signal is set at $\pi/3$.

The radio-frequency-transfer stability through an optical fiber network in terms of the Allan deviation is 3.4527×10^{-4} with an averaging time of 1s and 1.0921×10^{-5} with an averaging time of 1000s.

In order to filter out the optical sidebands resulting from the modulation process, we have used Butterworth filters as tunable optical filters. They are a type of signal processing filters designed to have a frequency response as flat as possible in the passband. The amplitude response of the nth Butterworth filter is given by

$$H(\omega) = \frac{1}{\sqrt{1 + (\omega/\omega_c)^{2n}}} \tag{20}$$

where n is the order of the filter and ω_c is the cut-off frequency.

When the modulation parameter of Mach-Zehnder modulators (m) and the extinction ratio (ER) of Mach-Zehnder modulators are modified, the frequency stability and, as a consequence, the Allan variance, changes.

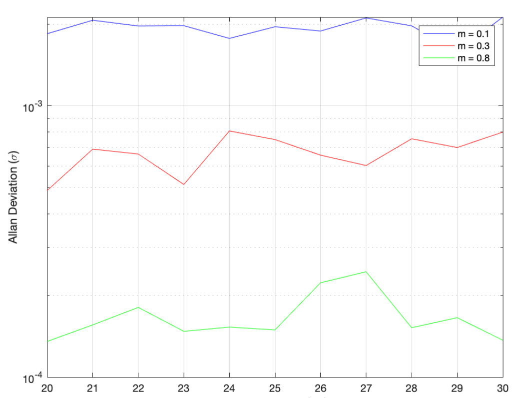

FIG. 6. Allan deviation as a function of extinction ratio in dB (ER) for different values of the modulation parameter of the third Mach-Zehnder modulator (m_3).

Fig. 6 shows the Allan deviation (σ) as a function of extinction ration in dB for different values of the modulation parameter of the third Mach-Zehnder modulator (m_3). The graph shows that the m_3 parameter is of utmost importance when very exact results are needed for any extinction ratio; and that the higher its value, the lower the deviation.

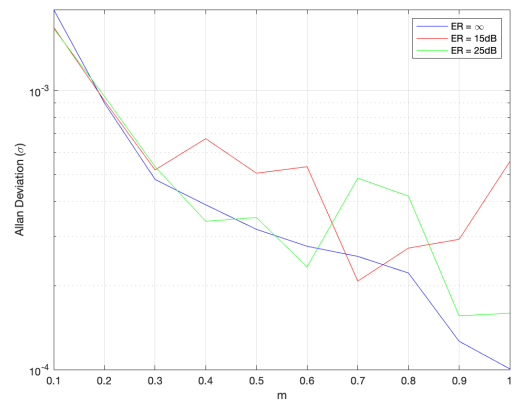

FIG. 7. Allan deviation as a function of the modulation parameter of the third Mach-Zehnder modulator (m_3) for typical values of the extinction ratio in dB (ER).

Fig. 7 shows the Allan deviation (σ) as a function of the modulation parameter of the third Mach-Zehnder modulator (m_3) for typical values of the extinction ratio in dB. From this data we can extract that, regardless of the extinction ratio the modulator is working with, the deviation will strongly depend on the aforementioned modulation parameter despite various evident fluctuations. Furthermore, we can also observe that, for small values of m_3, the Allan deviation is much more stable than for higher ones, also independently of the used ER.

V. CONCLUSIONS

We have proved that stable frequency dissemination with phase conjugation can be successfully implemented without using multipliers and mixers in the scheme, thus avoiding the local oscillator leakage and mixing spurs from mixers.

The results show that the proposed scheme is not only effective but also practical.

We have observed that phase conjugation can be affected by backward Rayleigh scattering [3] of the fiber link. This problem might be solved in future works.

VI. ACKNOWLEDGMENTS

We would like to thank María Santos Blanco for her assessment and kind help throughout the work.

[1] Wang, H., Xue, X., Li, S., and Zheng, X. (2018). All-optical arbitrary-point stable quadruple frequency dissemination with photonic microwave phase conjugation. IEEE Photonics Journal, 10(4), 1-8.

[2] Gozzard, D. R. (2017). A stabilized frequency reference transfer system for the square kilometre array.

[3] Liang, J., Liu, C., Hu, F., Zhou, S., Yu, S., and Qiao, Y. (2019). Stable radio-frequency dissemination system of single wavelength with passive compensation and remote reconstruction. Optics Communications, 445, 161-164.

[4] Yin, F., Zhang, A., Dai, Y., Ren, T., Xu, K., Li, J., ... and Tang, G. (2014). Phase-conjugation-based fast RF phase stabilization for fiber delivery. Optics express, 22(1), 878-884.

[5] Liao, L., Samara-Rubio, D., Morse, M., Liu, A., Hodge, D., Rubin, D., ... and Franck, T. (2005). High speed silicon Mach-Zehnder modulator. Optics express, 13(8), 3129-3135.

[6] Švarný, J. (2010, October). Analysis of quadrature bias-point drift of Mach-Zehnder electro-optic modulator. In 2010 12th Biennial Baltic Electronics Conference (pp. 231-234). IEEE.

[7] Yu, L., Wang, R., Lu, L., Zhu, Y., Wu, C., Zhang, B., a nd Wang, P. (2014). Stable radio frequency dissemination by simple hybrid frequency modulation scheme. Optics letters, 39(18), 5255-5258.

[8] Fujieda, M., Kumagai, M., Gotoh, T., and Hosokawa, M. (2008). Ultrastable frequency dissemination via optical fiber at NICT. IEEE Transactions on Instrumentation and Measurement, 58(4), 1223-1228.

[9] What is a Mach-Zehnder Modulator and How Does it Work? — Synopsys. (n.d.). Synopsis. Retrieved May 22, 2021, from https://www.synopsys.com/glossary/what-is-a-mach-zehnder-modulator.html

[10] Omomukuyo, O., Thakur, M., and Mitchell, J. (2012). Experimental demonstration of the impact of MZM non-linearity on direct-detection optical OFDM. 2012 IEEE Wireless Communications and Networking Conference (WCNC), 3753-3757.

Appendix A: Code to plot the dependence of Allan deviation on the extinction ratio (ER)

```
%% STABLE RADIO-FREQUENCY DISSEMINATION WITH PHASE CONJUGATION
%% Allan deviation as a function of ER for different values of m

% A typical extinction ratio of commercially available MZ
% (Mach-Zehnder) intensity modulators lies in the range 20-30dB

SR = 2^10; % Sampling rate with units of GHz (power of two)
TW = 2^10; % Time window with units of ns

N = TW*SR; % Number of samples

t = [0:(1/SR):(TW-1/SR)];
f = [0:(1/TW):(SR-1/TW)];

f_plot  = [-SR/2:(1/TW):(SR/2-1/TW)];

phi0 = 4*pi/9; % Initial phase of the RF signal
f_RF = 1; % Initial frequency of the RF signal

m3 = [0.1 0.3 0.8];

% Extinction Ratio

ER = 20:30;
gamma = [];

for k = 1:length(ER)

gamma(k) = (10^(ER(k)/20)-1)/(10^(ER(k)/20)+1);

end

avar = zeros(length(m3),1);

allan = zeros(length(m3),length(gamma));

% MZM parameters in push-pull configuration

b1 = 3*pi/2; % Bias angle at null point
m1 = 0.8; % Modulation parameter

b2 = 3*pi/2; % Bias angle at null point
m2 = 0.8; % Modulation parameter

b3 = 7*pi/4; % Bias angle at quadrature point



for ii = 1:length(gamma)

for jj = 1:length(m3)

% INPUT: RF signal generated by a microwave source

V1_t = cos(2*pi*f_RF*t + phi0);
V1_f = (1/N)*fftshift(fft(fftshift(V1_t)));

% E1 is modulated by the RF signal V1 at MZM1

E1_t = cos(b1 + m1*V1_t);
E1_f = (1/N)*fftshift(fft(fftshift(E1_t)));
E1_f = 0.5*E1_f/abs(E1_f(f_plot==1));

% TOF1 (Buttherworth Filter)

fc1 = 1.9; n = 4;
```

```
H_f1 = 1./(1+(f_plot/fc1).^(2*n));

E1_fil = E1_f.*H_f1;
E1_fil = 0.5*E1_fil/abs(E1_fil(f_plot==1));
E1_fil_t = N*ifftshift(ifft(ifftshift(E1_fil)));

% Then, E1 is divided into two branches through an optical coupler
% (OC1). One branch is transmitted along a single mode fiber (SMF1)
% to the remote site.

tau1 = rand(1); % Forward propagation through fiber with a random phase
E2_f = E1_fil.*exp(-1i*2*pi*f_plot*tau1);
E2_f = 0.5*E2_f/abs(E2_f(f_plot==1));
E2_t = N*ifftshift(ifft(ifftshift(E2_f)));

% The other branch is photodetected by PD1 and a frequency-doubled
% RF signal is obtained.

V2_t = abs(E1_fil_t).^2;
V2_f = (1/N)*fftshift(fft(fftshift(V2_t)));
V2_f(f_plot==0) = 0; % Removing the continuous component in frequency domain
V2_f = 0.5*V2_f/abs(V2_f(f_plot==2));
V2_t = N*ifftshift(ifft(ifftshift(V2_f))); % Applying the removing of the continuous component

% At the remote site 1, the OC2 couples out a forward transferred
% optical signal denoted by E2. The other part is injected into SMF2
% and returns to the local site as a round-trip probe signal. The
% round-trip probe signal E3 is written as:

tau2 = rand(1); % Forward propagation through fiber with a random phase
E3_f = E2_f.*exp(-1i*2*pi*f_plot*tau2);
E3_f = 0.5*E3_f/abs(E3_f(f_plot==1));
E3_t = N*ifftshift(ifft(ifftshift(E3_f)));

% E3 is modulated by the frequency-doubled signal V2 at MZM2

E4_t = E3_t.*cos(b2 + m2*V2_t);
E4_f = (1/N)*fftshift(fft(fftshift(E4_t)));
E4_f = 0.5*E4_f/abs(E4_f(f_plot==1));

% TOF2 (Buttherworth Filter)

fc2 = 2; n = 8;
H_f2 = 1./(1+(f_plot/fc2).^(2*n));

E4_fil = E4_f.*H_f2;
E4_fil = 0.5*E4_fil/abs(E4_fil(f_plot==1));
% E4_fil_t = N*ifftshift(ifft(ifftshift(E4_fil)));

% The signal E4 is propagated backward to the remote site along
% SMF2. The forward and backward signals transmitted over SMF2
% undergo the same propagation delay.

% Backward propagation through fiber with a random phase

E5_f = E4_fil.*exp(-1i*2*pi*f_plot*tau2);
E5_f = 0.5*E5_f/abs(E5_f(f_plot==1));
E5_t = N*ifftshift(ifft(ifftshift(E5_f)));

% After photodetection by PD2, the phase-conjugation RF signal is:

V3_t = abs(E5_t).^2;
V3_f = (1/N)*fftshift(fft(fftshift(V3_t)));
V3_f(f_plot==0) = 0;
V3_f = 0.5*V3_f/abs(V3_f(f_plot==2));
V3_t = N*ifftshift(ifft(ifftshift(V3_f)));

% E2 is modulated by the frequency-doubled signal V3 at MZM3 biased
% at quadrature point
```

```
E6_t = E2_t.*(exp(1i*(b3+m3(jj)*V3_t)./2)+gamma(ii)*exp(-1i*(b3+m3(jj)*V3_t)./2));
% E6_f = (1/N)*fftshift(fft(fftshift(E6_t)));
% E6_f = 0.5*E6_f/abs(E6_f(f_plot==1));

V4_t = abs(E6_t).^2;
V4_f = (1/N)*fftshift(fft(fftshift(V4_t)));
V4_f = 0.5*V4_f/abs(V4_f(f_plot==4));

%{

k =  [find(f_plot==-3) find(f_plot==3)];
j = [find(f_plot==-5) find(f_plot==5)];

V4_f(k(1):k(2)) = 0;
V4_f(1:j(1)) = 0;
V4_f(j(2):end) = 0;

%}

% V4_t = N*ifftshift(ifft(ifftshift(V4_f)));

avar(jj) = allanvar(abs(V4_f),10^3);

end

allan(:,ii) = avar;

end

figure(1)
semilogy(ER,sqrt(allan(1,:)),'b')
hold on
semilogy(ER,sqrt(allan(2,:)),'r')
semilogy(ER,sqrt(allan(3,:)),'g')
xlabel('Extinction Ratio (dB)')
ylabel('Allan Deviation (\sigma)')
legend('m = 0.1','m = 0.3','m = 0.8')
grid on
```

Appendix B: Code to plot the dependence of Allan deviation on the modulation parameter (m_3)

```
%% STABLE RADIO-FREQUENCY DISSEMINATION WITH PHASE CONJUGATION
%% Allan deviation as a function of m for different values of ER

SR = 2^10; % Sampling rate with units of GHz (power of two)
TW = 2^10; % Time window with units of ns

N = TW*SR; % Number of samples

t = [0:(1/SR):(TW-1/SR)];
f = [0:(1/TW):(SR-1/TW)];

f_plot  = [-SR/2:(1/TW):(SR/2-1/TW)];

phi0 = 4*pi/9; % Initial phase of the RF signal
f_RF = 1; % Initial frequency of the RF signal

% Extinction Ratio

gamma =  @(ER) (10^(ER/20)-1)/(10^(ER/20)+1);

gamma = [1 gamma(15) gamma(25)];

avar = zeros(length(gamma),1);

allan = zeros(length(gamma),10);

% MZM parameters in push-pull configuration

b1 = 3*pi/2; % Bias angle at null point
m1 = 0.8; % Modulation parameter

b2 = 3*pi/2; % Bias angle at null point
m2 = 0.8; % Modulation parameter

b3 = 7*pi/4; % Bias angle at quadrature point

m3 = 0.1:0.1:1;

for jj = 1:length(m3)

for ii = 1:length(gamma)

% INPUT: RF signal generated by a microwave source

V1_t = cos(2*pi*f_RF*t + phi0);
V1_f = (1/N)*fftshift(fft(fftshift(V1_t)));

% E1 is modulated by the RF signal V1 at MZM1

E1_t = cos(b1 + m1*V1_t);
E1_f = (1/N)*fftshift(fft(fftshift(E1_t)));
E1_f = 0.5*E1_f/abs(E1_f(f_plot==1));

% TOF1 (Buttherworth Filter)

fc1 = 1.9; n = 4;
H_f1 = 1./(1+(f_plot/fc1).^(2*n));

E1_fil = E1_f.*H_f1;
E1_fil = 0.5*E1_fil/abs(E1_fil(f_plot==1));
E1_fil_t = N*ifftshift(ifft(ifftshift(E1_fil)));

% Then, E1 is divided into two branches through an optical coupler
% (OC1). One branch is transmitted along a single mode fiber (SMF1)
% to the remote site.
```

```
tau1 = rand(1); % Forward propagation through fiber with a random phase
E2_f = E1_fil.*exp(-1i*2*pi*f_plot*tau1);
E2_f = 0.5*E2_f/abs(E2_f(f_plot==1));
E2_t = N*ifftshift(ifft(ifftshift(E2_f)));

% The other branch is photodetected by PD1 and a frequency-doubled
% RF signal is obtained.

V2_t = abs(E1_fil_t).^2;
V2_f = (1/N)*fftshift(fft(fftshift(V2_t)));
V2_f(f_plot==0) = 0; % Removing the continuous component in frequency domain
V2_f = 0.5*V2_f/abs(V2_f(f_plot==2));
V2_t = N*ifftshift(ifft(ifftshift(V2_f))); % Applying the removing of the continuous component

% At the remote site 1, the OC2 couples out a forward transferred
% optical signal denoted by E2. The other part is injected into SMF2
% and returns to the local site as a round-trip probe signal. The
% round-trip probe signal E3 is written as:

tau2 = rand(1); % Forward propagation through fiber with a random phase
E3_f = E2_f.*exp(-1i*2*pi*f_plot*tau2);
E3_f = 0.5*E3_f/abs(E3_f(f_plot==1));
E3_t = N*ifftshift(ifft(ifftshift(E3_f)));

% E3 is modulated by the frequency-doubled signal V2 at MZM2

E4_t = E3_t.*cos(b2 + m2*V2_t);
E4_f = (1/N)*fftshift(fft(fftshift(E4_t)));
E4_f = 0.5*E4_f/abs(E4_f(f_plot==1));

% TOF2 (Buttherworth Filter)

fc2 = 2; n = 8;
H_f2 = 1./(1+(f_plot/fc2).^(2*n));

E4_fil = E4_f.*H_f2;
E4_fil = 0.5*E4_fil/abs(E4_fil(f_plot==1));
% E4_fil_t = N*ifftshift(ifft(ifftshift(E4_fil)));

% The signal E4 is propagated backward to the remote site along
% SMF2. The forward and backward signals transmitted over SMF2
% undergo the same propagation delay.

% Backward propagation through fiber with a random phase

E5_f = E4_fil.*exp(-1i*2*pi*f_plot*tau2);
E5_f = 0.5*E5_f/abs(E5_f(f_plot==1));
E5_t = N*ifftshift(ifft(ifftshift(E5_f)));

% After photodetection by PD2, the phase-conjugation RF signal is:

V3_t = abs(E5_t).^2;
V3_f = (1/N)*fftshift(fft(fftshift(V3_t)));
V3_f(f_plot==0) = 0;
V3_f = 0.5*V3_f/abs(V3_f(f_plot==2));
V3_t = N*ifftshift(ifft(ifftshift(V3_f)));

% E2 is modulated by the frequency-doubled signal V3 at MZM3 biased
% at quadrature point

E6_t = E2_t.*(exp(1i*(b3+m3(jj)*V3_t)./2)+gamma(ii)*exp(-1i*(b3+m3(jj)*V3_t)./2));
% E6_f = (1/N)*fftshift(fft(fftshift(E6_t)));
% E6_f = 0.5*E6_f/abs(E6_f(f_plot==1));

V4_t = abs(E6_t).^2;
V4_f = (1/N)*fftshift(fft(fftshift(V4_t)));
V4_f = 0.5*V4_f/abs(V4_f(f_plot==4));

%{
```

```
k =  [find(f_plot==-3) find(f_plot==3)];
j = [find(f_plot==-5) find(f_plot==5)];

V4_f(k(1):k(2)) = 0;
V4_f(1:j(1)) = 0;
V4_f(j(2):end) = 0;

%}

% V4_t = N*ifftshift(ifft(ifftshift(V4_f)));

avar(ii) = allanvar(abs(V4_f),10^3);

end

allan(:,jj) = avar;

end

figure(1)
semilogy(m3,sqrt(allan(1,:)),'b')
hold on
semilogy(m3,sqrt(allan(2,:)),'r')
semilogy(m3,sqrt(allan(3,:)),'g')
xlabel('m')
ylabel('Allan Deviation (\sigma)')
legend('ER = \infty','ER = 15dB','ER = 25dB')
grid on
```